Asian Journal of Chemistry; Vol. 33, No. 11 (2021), 2774-2780

ASIAN JOURNAL OF CHEMISTRY

https://doi.org/10.14233/ajchem.2021.23385

Fabrication of Substituted-Hydroxyapatite/Poly(vinyl pyrrolidone)-Poly(methyl methacrylate) Biocomposites for Bone Tissue Engineering Applications

G. PRIYA[1,2,*] and N. VIJAYAKUMARI[1]

[1]Department of Chemistry, Government Arts College for Women, Salem-636008, India
[2]Department of Chemistry, Shri Sakthikailassh Women's College, Salem-636003, India

*Corresponding author: E-mail: priya88chemistry@gmail.com

Received: 26 June 2021; *Accepted*: 23 August 2021; *Published online*: 20 October 2021; AJC-20562

Present work based on the development and incorporation of zinc-cerium substituted hydroxyapatite (ZCHA) nanoparticles into the host material of the dual polymer blend of poly(vinyl pyrrolidone) (PVD)-poly(methyl methacrylate) (PMMA). Numerous characterization techniques such as FTIR, XRD and SEM-EDX have been used in morphological and structural investigations of prepared nanoparticles and ZCHA reinforced PMMA-PVD biocomposites. The mechanical properties of ZCHA/PVD-PMMA biocomposites, like compressive strength was evaluated. To examine the biocompatibility of biocomposites, hemocompatibility experiments have been carried out. The antimicrobial activities of biocomposites toward Gram-positive and Gram-negative bacteria have also been tested and the cytotoxic existence of biocomposites has been evaluated using the MTT assay experiment. The developed ZCHA/PVD-PMMA biocomposites is suggested to provide the finest medicinal benefits in the application of biomaterials.

Keywords: Bone, Biocomposite, Hydroxyapatite, Poly(vinyl pyrrolidone), Poly(methyl methacrylate), Cerium, Zinc.

INTRODUCTION

Bone is a heavily vascularized tissue worth the effort to renovate and thereby protect the integrity of the skeleton in its traditional architecture [1,2]. Not only does this good tissue offer a structure for the bone, it also acts as a nutrient and plasma production reservoir. Nevertheless, treatments are needed in cases with bone fractures such as accident, sarcomas, osteomyelitis, *etc*. where normal bone recovery does not occur naturally [3,4]. Tissue engineering research has been very sophisticated in that it often uses bioceramics, polymers, metals and alloys as components for insertion applications. Among the most intelligently used bioceramic components is hydroxyapatite, which is the main inorganic portion of teeth and bones, and has outstanding osteogenic and osteoinduction characteristics [5]. In comparison, synthetic hydroxyapatite and human bone exhibit close interaction to those of natural aspect. When substituted with zinc and cerium minerals, hydroxyapatite offers excellent antimicrobial activity and much more reactivity contrasted to other metal biomaterials [6,7]. Despite these characteristics of hydroxyapatite, it is considered to have low compressive performance and thus can only be a binding material or as a biocomposite with other biomaterials.

A biocomposite is most often treated as a substance that combines the bioceramic nanoparticles' toughness, stiffness and durability and the polymer matrix's plasticity and availability [8]. PMMA has been extensively used in the therapy of fracture fractures and surgical regeneration of bones among many polymeric materials [9]. It is a non-degradable, continuous thermoplastic, which has long-term use as an embedded product [10]. Conversely, it can be used along with many other polymeric materials such as chitosan, poly(vinyl pyrrolidone), polystyrene, polysulfones, poly-ε-caprolactone, *etc.* owing to its low mechanical properties and weak bind to the bone. Due to its fascinating absorption and dynamic capacity, polyvinyl pyrrolidone (PVD) has strong stature. Like synthetic polymers, PVD is soluble in water. Also mentioned was the use of PVD in medication and treatments on the skin for drug delivery systems [11]. Consequently, with other polymers, it is understood that different complexes emerge [12].

The strengthening of zinc-cerium substituted hydroxyapatite (ZCHA) in the PVD-PMMA matrix is intended to enhance the mechanical properties and improve biomimetic, antimicrobial and biocompatible characteristics in the produced biocomposite materials. There are many methods for dispersing ZCHA into the matrix material; it is exceedingly difficult to spread the ZCHA uniformly into the polymer matrices. The present work describes solvent evaporation as a comfortable way to introduce ZCHA integrated PVD-PMMA biocomposites. While the distribution of ZCHA nanoparticles into PVD-PMMA framework needs antimicrobial and bioactive characteristics in the intended substance, the use of hydrophobic (PMMA) and hydrophilic (PVD) polymers implies that the produced material has the necessary compressive performance. Therefore, aiming at the importance of polymer based biocomposites in biomedical applications, the current work focuses on the fabrication of antimicrobial biocomposites of ZCHA/PVD-PMMA and the analysis of their physico-chemical and biological properties.

EXPERIMENTAL

Preparation of zinc-cerium substituted hydroxyapatite (ZCHA) nanoparticles: Substituted hydroxyapatite powders have been prepared using a typical neutralization path [13]. The analytical proportions (Ca + M)/P (where M = Sr + Zn) were held at 1.67. Beginning suspension was primed by dissolving calcium nitrate, zinc nitrate or cerium nitrate in double distilled water. The aqueous phase of phosphoric acid was used as an origin of phosphate and was applied to the beginning phase at a reasonable pace of introduction. The pH of the formulation solution was maintained at about 9 with a 25 % NH_3 solution. The temperatures of the reaction were kept constant at 50 ºC. The precipitates collected were left to grow overnight, purified and cleaned with double distilled water. After this, the precipitates were sintered at 450 ºC for 4 h, grinded and carefully sieved to fine powders.

Fabrication of ZCHA/PVD-PMMA biocomposites: Solvent evaporation technique was used for the fabrication of ZCHA-polymer biocomposites from many processing techniques [14]. In a standard procedure, PVD and PMMA of 1:1 w/w ratios were soluble in 50 mL chloroform and held for shaking until all the composites were fully dissolved. Subsequently, specific weights of ZCHA were applied to the corresponding composite samples of polymeric materials. The uniform diffusion of ZCHA nanoparticles in a polymeric mixture was preserved for mixing up to 12 h. In order to evaporate the solvent, the liquid was drained onto a petri-plate. The solutions for the various formulations designed are summarized in Table-1. Biocomposite films were stripped off, cleaned with purified cleaned to prevent residual solvent and residual contaminants and gradually dried in the oven for 2 days. The filtered and cured biocomposites film was processed or used for future analyses.

TABLE-1
DATA SHOWED DIFFERENT FORMULATIONS OF BIOCOMPOSITES

Composite	ZCHA (g)	PVP (g)	PMMA (g)
Composite (PVP-PMMA)	–	1	1
Composite-1 (C-1)	1	1	1
Composite-2 (C-2)	2	1	1
Composite-3 (C-3)	3	1	1

Characterization: The FTIR analysis was performed on prepared samples using FTIR Bruker Vertex. The XRD patterns of prepared samples were reported using the D8 Advance X-ray diffractometer. The microstructure of the prepared samples was studied to use the JSM-SEM device.

Mechanical test: The compressive characteristic of the prepared samples were calculated at room temperature using a universal test machine (Instron) with 50 N load cell [15]. Dry spherical samples with a length of 25 mm and a width of 12 mm were used as experimental samples and condensed at a rate of 0.7 mm/min. The process finished with a 50% strain of the specimens. The modulus (E) was measured as the stress *vs*. the strain curve at 5% of the vertical area stress. The sum of both findings was three tests.

Swelling study: The degree of swelling was measured using the traditional gravimetric procedure [16]. The tests were carried out by taking before weighed specimens and placing them in a phosphate buffer for swollen to various time periods before the balance swelling was achieved, after the specimens had been withdrawn from the solution, pressed between each one two absorbent paper to dry it and eventually weighed.

Protein adsorption: In addition to identifying the relationship between both the specimens and the blood plasma, a protein adsorption technique was accompanied by adsorbent of the BSA protein to the interfaces of the prepared samples [17]. A freshly BSA formulation was made in 0.5 M PBS and the samples were then placed in a PBS oven for 1 day. Subsequently, the BSA mixture composed of pre-weighed and completely swollen nanomaterials and polymer components was refluxed for 3 h. To prevent the formation of foam in the protein solution, stirring was performed softly, because BSA could reabsorb at the surface of air-protein solution. Since stirring, the residual centrifuging protein solution was discarded BSA intensity was measured by measuring the absorption spectrum on the spectrophotometry.

Hemocompatiblity test: Haemolysis induced by prepared compound has been examined using a methodology given elsewhere [18].

Antibacterial activity: Test specimens of various formulations were measurably inspected for antimicrobial properties using a disc-diffusion system toward Gram-positive and Gram-negative bacteria. Bactericidal induced by prepared samples substances has been documented using a known methodology [19].

Viability assay: The MTT assay procedure was used to determine the viability of the prepared samples. The osteoblast was implanted to a culture microplate (5×10^4 cell/well) composed of 1 mL of DMEM. Cells (5% CO_2, 37 ºC) were cultured for one day the medium was extracted and DMEM was applied about each well, consisting of specimens of a particular substance extract. The extraction composed of DMEM medium was then combined with 1 mL of fresh DMEM and additional cells were culture overnight for 1, 3 and 7 days, respective. At

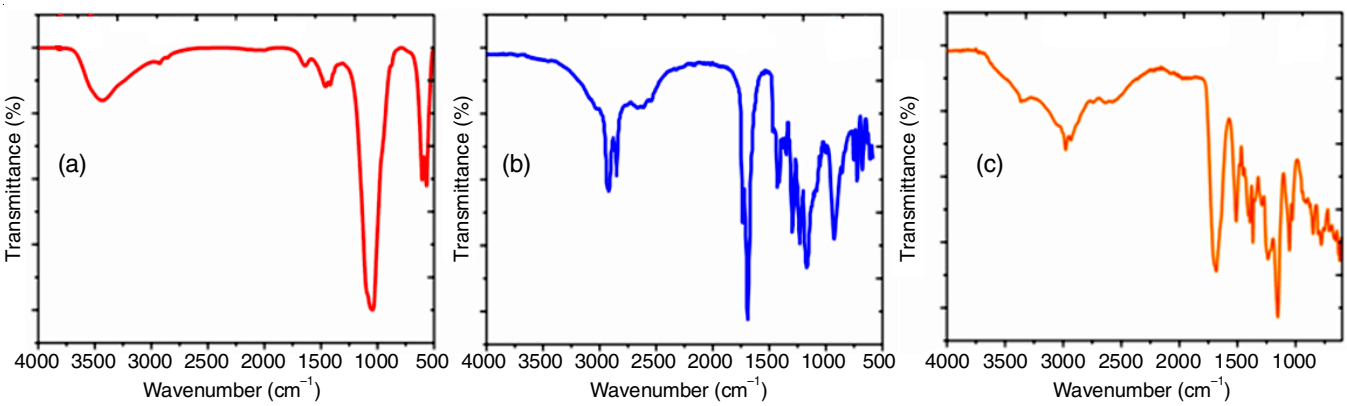

Fig. 1. FTIR spectra of (a) ZnHA, (b) PVD-PMMA and (c) ZCHA/PVD-PMMA biocomposites

last a 60 µL formulation of MTT in DMEM was applied to every sample. Upon culturing for 6 h, the solution of MTT was removed of each medium; 2 mL of DMSO was applied from each well and then further cultivated at room temperature for one day with moderate stirring in the night. The optical density was registered on the microplate reader at 570 nm.

RESULTS AND DISCUSSION

FTIR spectra: The FTIR spectra of ZCHA, PVD-PMMA and ZCHA strengthened PMMA-PVD biocomposites are shown in Fig. 1a-c, respectively. The characteristic 3436 cm^{-1} absorption peak is due to OH^- group stretching vibrations are seen in Fig. 1a. The absorption peaks are the typical bands for the phosphate group at around 1058 cm^{-1} and 603 cm^{-1} and the peaks around 623 cm^{-1} and 3436 cm^{-1} are due to the hydroxy group's stretching and vibration modes, respectively thereby supporting the development of the ZCHA phase (Fig. 1a) [20]. PVD-PMMA and ZCHA packed biocomposite FTIR spectra are given in Fig. 1b-c, respectively. Furthermore, the peaks at 2930, 1718, 1412, 1230, 1161, 912 and 816 cm^{-1} corresponding to the PVD-PMMA are adsorbed on the surface of ZCHA [21]. In Fig. 1c, which shows the introduction of ZCHA into the PVD-PMMA matrix, the spectrum bands are changed. The biocomposite FTIR spectra revealed the substantial peaks of both ZCHA and PVD-PMMA, showing the mixing of ZCHA with PVD-PMMA.

XRD: Fig. 2a-b displays the XRD patterns of ZCHA and biocomposite, respectively. As shown by standard JCPDS file no 09-0432 [21], typical X-ray diffraction patterns of prepared ZCHA and biocomposite closely fit in phases. Typical planes at 2θ values of 26º (002), 31º (211), 32º (112) and 34º (200) are observed in the X-ray diffraction patterns range of ZCHA particles seen in Fig. 2a, which are identical to the planes observed in Fig. 2b. The PVD-PMMA in biocomposite has been shown to peak about 21º, angle for PVD and the hump at 10.9º, angle assigned to PMMA when evaluated in Fig. 2b [22]. The XRD results show that the properties of apatite with a strong crystalline structure are displayed by ZCHA and also mean there are no impurities or phase transition.

SEM: In Fig. 3a-d, accordingly, a typical SEM illustration of pure PVD-PMMA, biocomposite specimens of separate ZCHA compositions were seen. As shown in Fig. 3a, ZCHA

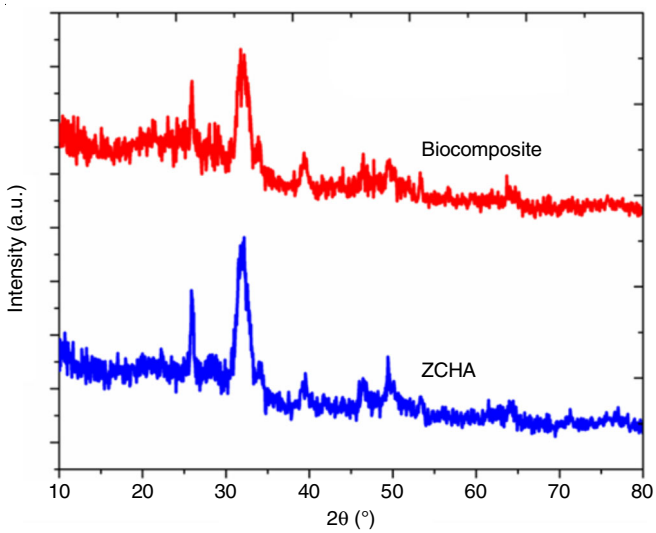

Fig. 2. XRD spectra of (a) ZnHA, (b) PVD-PMMA and (c) ZCHA/PVD-PMMA biocomposites

nanoparticles have been synthesized as flaks particles. It is evident from Fig. 3b that the structure of the flakes morphology with the smooth texture was detected by pure PVD-PMMA. The microstructure of the biocomposites, on the other hand, showed substantial surface quality with sufficient bumped and clustered compositions, which increased dramatically to 3% with ZCHA nanoparticles (Fig. 3c-e). Therefore, the morphology of biocomposites is somewhat distinct from that of pure films. The enhanced uniformity is the result of massive mixtures of the polymer chains as published elsewhere [23]. Bioceramic nanoparticles may strengthen the polymer matrix sequence either by holding specific results at certain periods, or by the edge in the polymer matrix, or by superimposing with one another [24,25].

Mechanical properties analysis: In dry conditions, a strength properties study of biocomposites was conducted to determine the mechanical strength of ZCHA/PVD-PMMA biocomposites (Fig. 4a-b). The result shows that the importance of compressive modulus and strength also raises as the sum of ZCHA rises. It is, therefore, obvious that the mechanical properties of ZCHA loaded PVD-PMMA is higher compared to the pure PVD-PMMA. The addition of ZCHA increases the mechanical characteristics of biocomposite, which is attributed

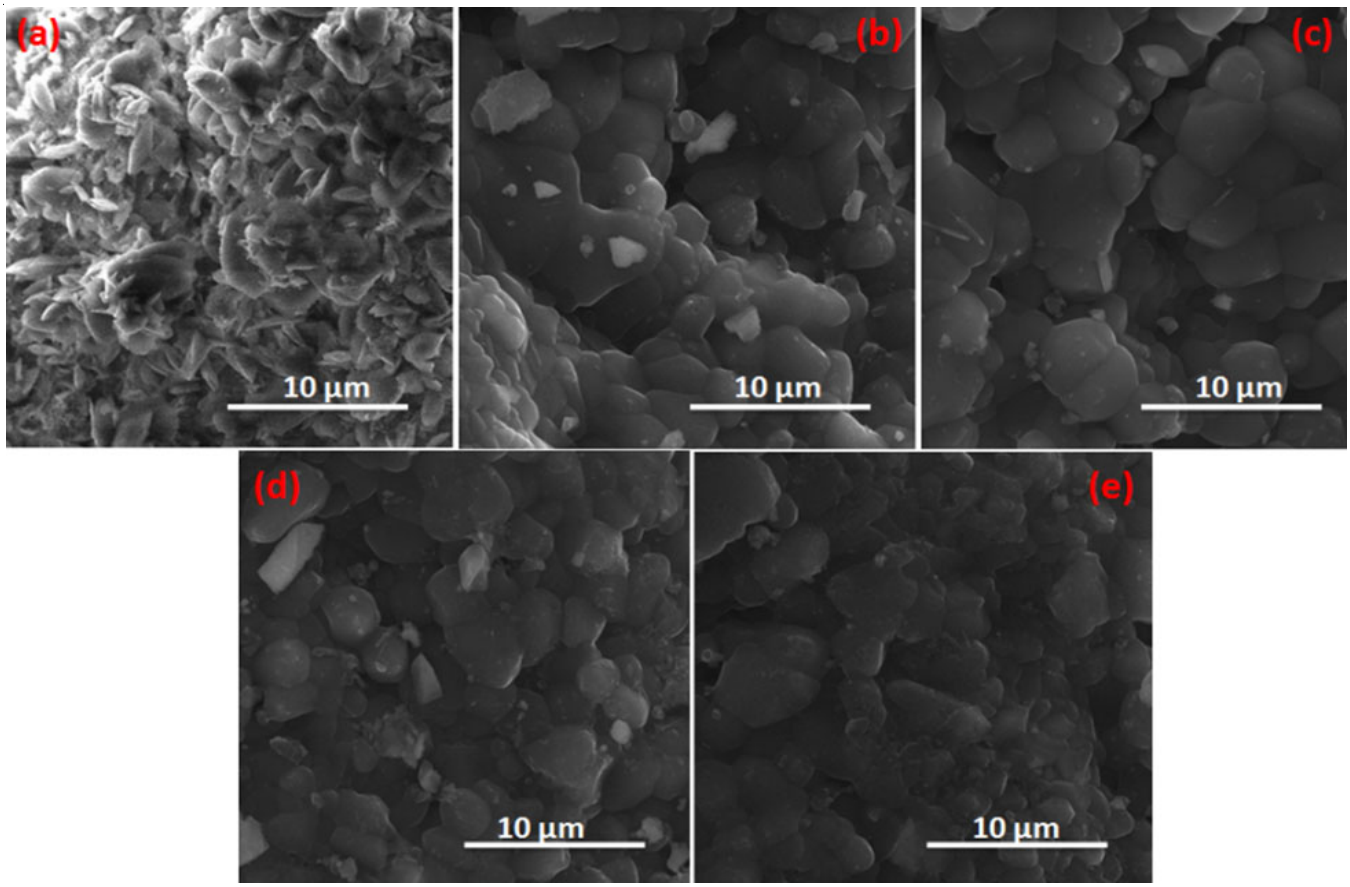

Fig. 3. SEM images of (a) ZnHA, (b) PVD-PMMA and (c-e) ZCHA/PVD-PMMA biocomposites

to the reason that the higher the proportion of the bioceramic to the polymeric materials, the larger the contact between the bioceramic (ZCHA) and the polymer matrix. The findings show that biocomposites may be used as tissue engin-eering of strong osteoconductivity. Results also suggest that whenever the volume of ZCHA is increased above 2 g, the compressive intensity and modulus of biocomposites decrease to 72 MPa. This may be attributed to the differentiation of ZCHA in the PVD-PMMA composite. As the amount of ZCHA rises, the uniformity of the composite is impaired, resulting in the decreased mechanical characteristics.

Swelling assay: A polymer matrix that consumes a suffi-cient volume of water displays growing tissues such as metabolic resilience, resemblance, reduced surface stress, membrane protein absorption, *etc*. [26,27]. The PVD-PMMA composite swelling activity was contrasted with that of ZCHA/PVD-PMMA biocomposites. The introduction of ZCHA into the PVD-PMMA matrix leads to a major improvement in the

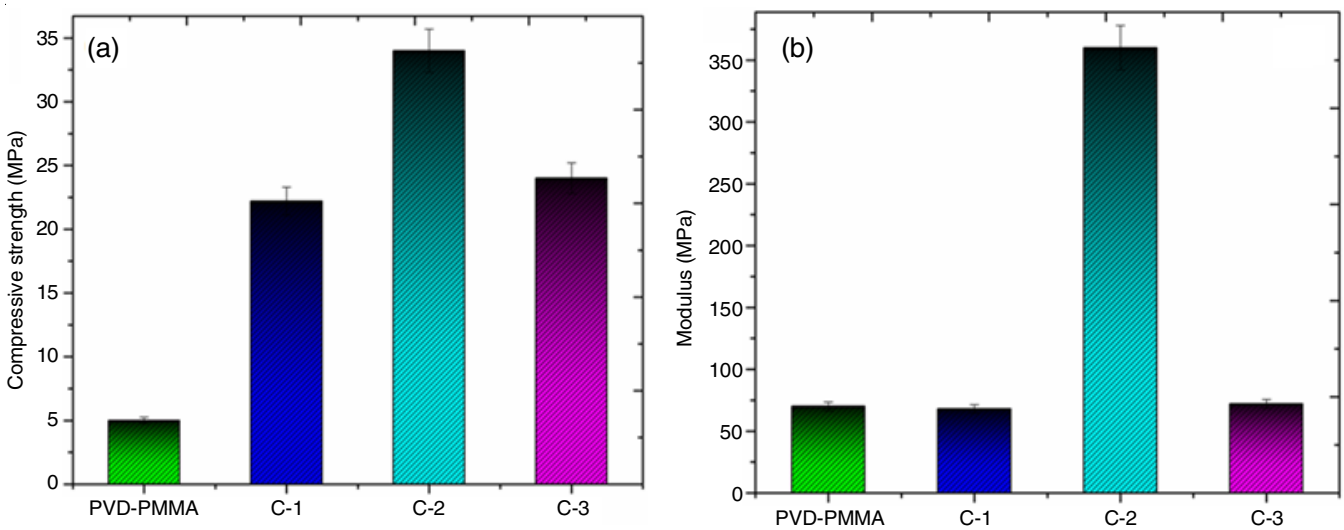

Fig. 4. (a) Compressive strength and (b) compressive modulus of prepared samples

function of the matrix's absorption and mechanical characteristics. The volume of ZCHA ranged from 1 to 3 g to test the impact of ZCHA on the swelling of the biocomposites. The swelling results outlined in Fig. 5 indicate that the swelling ratio declines as the volume of ZCHA increases. The decline in the swelling ratio is responsible for the increase in the association between the PVD-PMMA matrix and ZCHA, which limits the movement of the PVD-PMMA matrix and decreases the swelling of biocomposites [28].

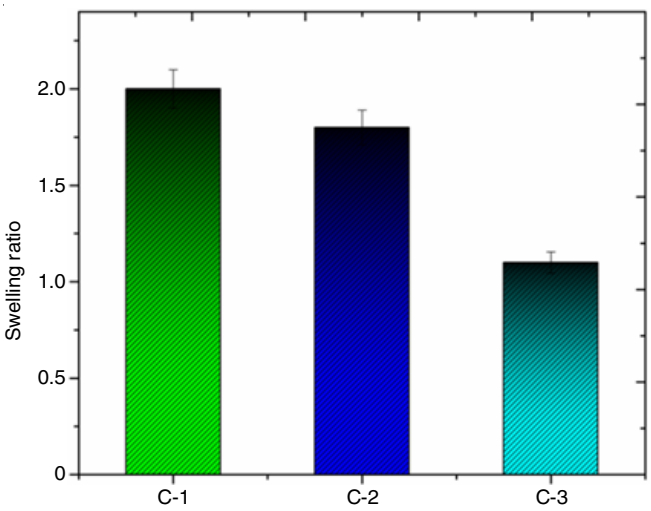

Fig. 5. Swelling ratio of prepared ZCHA/PVD-PMMA biocomposites

Protein adsorption assay: The biocompatibility of the fabricated ZCHA and ZCHA/PVD-PMMA biocomposites was examined through the adsorption of protein to the interfaces of the biocomposites. The larger adsorption of protein to ZCHA can be related to the fact that fast ion reactions between phosphate and calcium ions of ZCHA and NH_4^+ cations and COO^- anions of a protein molecule, a large proportion of protein biomolecules are adsorbed to bioceramic substrates [29,30]. The results also show that as ZCHA levels are increased in the range studied, protein adsorption is steadily growing (Fig. 6).

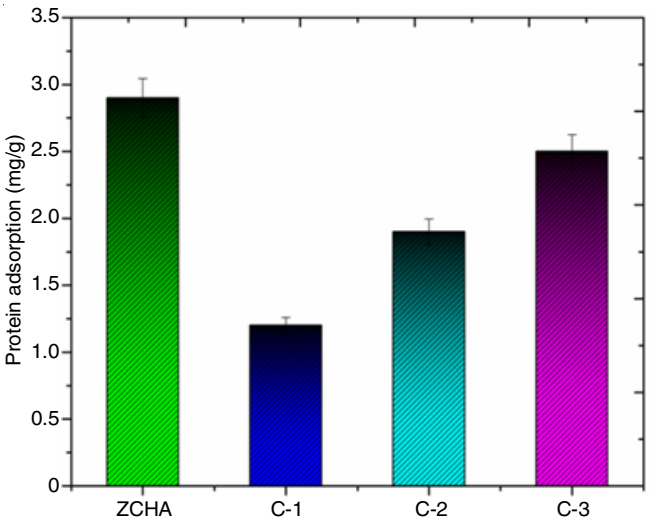

Fig. 6. Protein adsorption of prepared ZCHA and ZCHA/PVD-PMMA biocomposites

The improvement found with increasing concentrations of ZCHA can be attributed to the fact that it is well understood that superior surfaces have a strong connection for adsorption and thus as the biocomposite incorporates more ZCHA, stronger adsorption is detected [31].

Hemocompatibility assay: Fig. 7 presents the findings of hemolytic experiments conducted on the surfaces of biocomposites of various formulations. Fig. 7 shows that the hemolysis is continuously decreasing with the increasing amount of ZCHA in the composite. These findings are attributable to ZCHA, which causes the strong linkages with protein complexes and contributes to decrease hemolysis. When the percentage hemolysis calculated value with the ZCHA blend of a certain formulation is contrasted with that observed with biocomposite, it is observed that the PVD-PMMA film induces more hemolysis than that induced by the biocomposite films. The low hemolysis achieved with biocomposite substances can be attributed to the fact that ZCHA is well established for its hemocompatible existence and thus its inclusion in the PVD-PMMA matrix contributes to a reduction in percentage hemolysis [32,33].

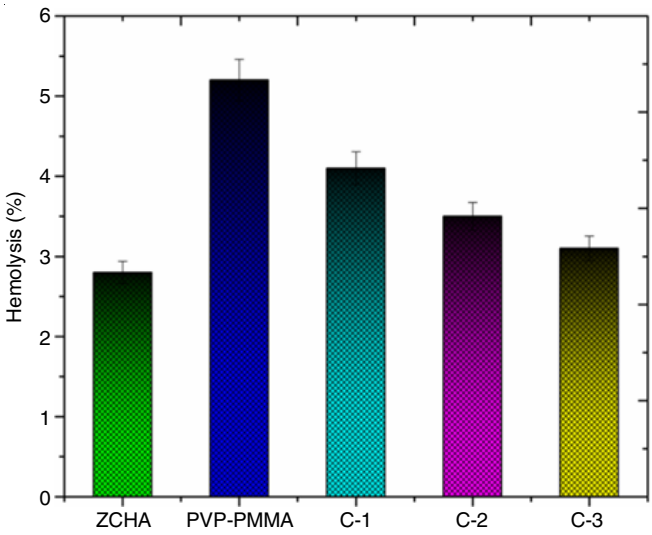

Fig. 7. Hemocompatibility assay of prepared ZCHA, PVD-PMMA and ZCHA/PVD-PMMA biocomposites

Antibacterial activity: Antibacterial protection tests for fabricated PVD-PMMA and biocomposites were conducted against Gram-positive and Gram-negative bacteria. From Fig. 8, it is clear that ZCHA biocomposites have bacteria destroying properties. The inhibition area for the specimens ZCHA/PVD-PMMA toward *S. aureus* and *E. coli* was observed to be increasing with an increased concentration of ZCHA. The antimicrobial effects demonstrated by ZCHA/PVD-PMMA biocomposite are due to the presence of cerium and zinc. The antimicrobial nature of silver has been reported in several studies [34,35].

Cell viability test: Cell viability of biocomposites was investigated by evaluating the feasibility of osteoblast cells as seen in Fig. 9. It was observed that the native PVD-PMMA composite film displayed weaker cell viability compared to ZCHA loaded biocomposites. The improvement in viable cells after 7th day of culturing suggests the development of cell growth. Furthermore, it was also found that the increase in the

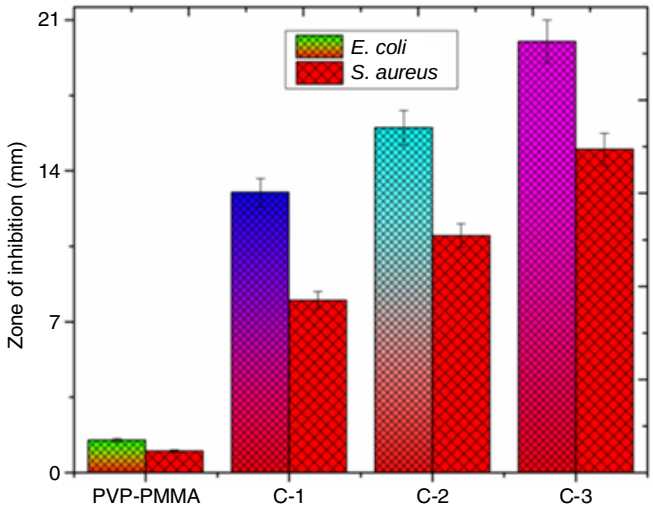

Fig. 8. Antibacterial activity of prepared PVD-PMMA and ZCHA/PVD-PMMA biocomposites

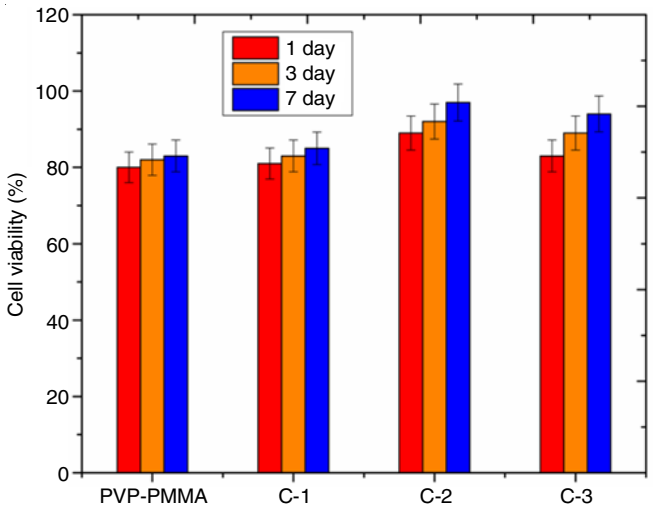

Fig. 9. Cell viability of prepared PVD-PMMA and ZCHA/PVD-PMMA biocomposites

percentage of ZCHA lowers viable cells due to a raise in the amount of Zn and Ce ions. PMMA is considered to have some hazards although PVD is bioactive. PVD-PMMA composite is thus of a somewhat toxic, while PMMA is of a much more toxic nature due to the inclusion of certain residual monomers. It has also been observed that up to 2 g of ZCHA content in biocomposites, the feasibility of osteoblast cells is much more than 80%, while after 7th day of ZCHA culturing, the feasibility of cells is more than 1st day, suggesting the cell growth.

Live/dead assay: Biocompatibility study of prepared samples was conducted to determine live/dead staining as shown in Fig. 10. Viable cells in green and damaged cells in red are seen in pictures of live/dead staining [36]. All groups registered improved cell growth on the seventh day relative to the 3rd day. Fig. 10 showed the live/death staining of biocomposites with the minimum dead cells and more living cells relative to PVD-PMMA. Live/dead assay findings indicate that most of the osteoblast cells in all biocomposite substances were live but one or some dead cells, while these biocomposites are healthy and suitable for osteoblast development. The findings of cell culture studies indicate that the biocomposite plays a crucial role in prosthetic devices.

Conclusion

In conclusion, novel biocomposites of zinc-cerium substituted hydroxyapatite (ZCHA) and poly(vinyl pyrrolidone) (PVD)-poly(methyl methacrylate) were developed by the solvent evaporation method and their mechanical characteristics and the biocompatibility were assessed. The spectroscopic and morphological analyses indicate excellently composite structures. The inclusion of ZCHA has shown an increase in the mechanical characteristics that'd be suitable for the clinical field. Biocomposites are non-toxic and have demonstrated good protein adsorption and cytocompatibility *in vitro*. In order to achieve the perfect biocompatible ZCHA/PVD-PMMA biocomposites for the fracture rehabilitation and replacement, further work is required that will show rapid advancements in the interaction between devices and biological tissue based on the information obtained from this work.

CONFLICT OF INTEREST

The authors declare that there is no conflict of interests regarding the publication of this article.

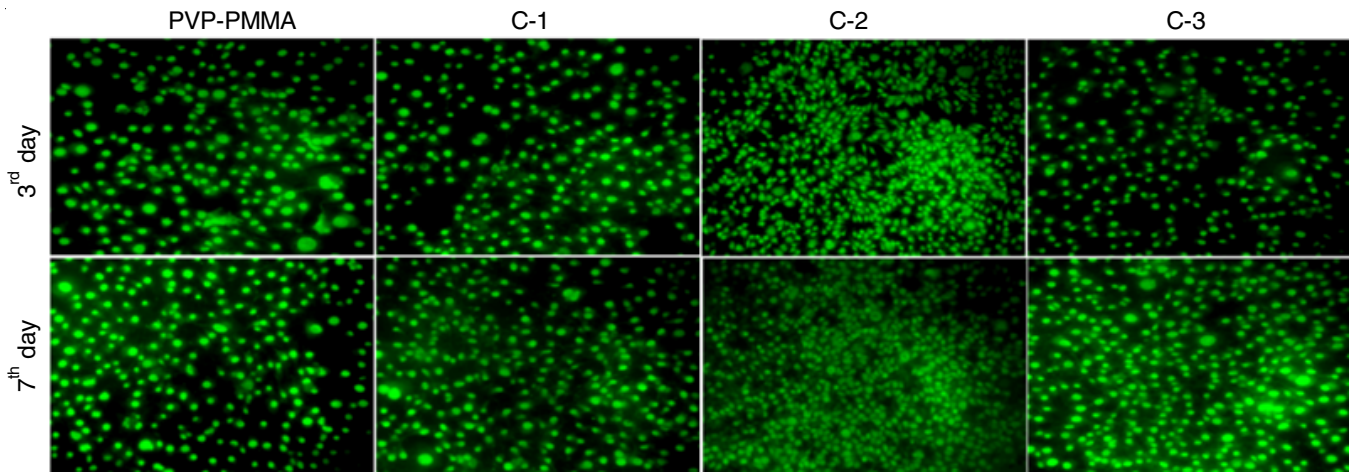

Fig. 10. Live/dead assay of prepared PVD-PMMA and ZCHA/PVD-PMMA biocomposites

REFERENCES

1. A.S. Neto and J.M. Ferreira, *Materials*, **11**, 1702 (2018); https://doi.org/10.3390/ma11091702
2. K. Hartmann, M. Koenen, S. Schauer, S. Wittig-Blaich, M. Ahmad, U. Baschant and J.P. Tuckermann, *Physiol. Rev.*, **96**, 409 (2016); https://doi.org/10.1152/physrev.00011.2015
3. J. Quinn, R. McFadden, C.W. Chan and L. Carson, *Iscience*, **23**, 101745 (2020); https://doi.org/10.1016/j.isci.2020.101745
4. A. Kashirina, Y. Yao, Y. Liu and J. Leng, *Biomater. Sci.*, **7**, 3961 (2019); https://doi.org/10.1039/C9BM00664H
5. G. Molino, M.C. Palmieri, G. Montalbano, S. Fiorilli and C. Vitale-Brovarone, *Biomed. Mater.*, **15**, 022001 (2020); https://doi.org/10.1088/1748-605X/ab5f1a
6. S. Wu, S. Ma, C. Zhang, G. Cao, D. Wu, C. Gao and S. Lakshmanan, *Saudi J. Biol. Sci.*, **27**, 2638 (2020); https://doi.org/10.1016/j.sjbs.2020.05.045
7. G. Priya, N. Vijayakumari and R. Sangeetha, *Adv. Mater. Devices*, **3**, 317 (2018); https://doi.org/10.1016/j.jsamd.2018.06.002
8. C. Shuai, L. Yu, P. Feng, C. Gao and S. Peng, *Biointerfaces*, **193**, 111083 (2020); https://doi.org/10.1016/j.colsurfb.2020.111083
9. J. Zhu, S. Yang, K. Cai, S. Wang, Z. Qiu, J. Huang, G. Jiang, X. Wang and X. Fang, *Theranostics*, **10**, 6544 (2020); https://doi.org/10.7150/thno.44428
10. Y.H. Li, X.Y. Shang and Y.J. Li, *Mater. Lett.*, **270**, 127744 (2020); https://doi.org/10.1016/j.matlet.2020.127744
11. M. Kurakula and G.S.N. Koteswara Rao, *Eur. Polym. J.*, **136**, 109919 (2020); https://doi.org/10.1016/j.eurpolymj.2020.109919
12. S.S. Garakani, S.M. Davachi, Z. Bagher, A.H. Esfahani, N. Jenabi, Z. Atoufi, M. Khanmohammadi, A. Abbaspourrad, H. Rashedi and M. Jalessi, *Int. J. Biol. Macromol.*, **164**, 356 (2020); https://doi.org/10.1016/j.ijbiomac.2020.07.138
13. C. Li and F. Meng, *Mater. Lett.*, **62**, 932 (2008); https://doi.org/10.1016/j.matlet.2007.07.013
14. S. Bodkhe, G. Turcot, F.P. Gosselin and D. Therriault, *ACS Appl. Mater. Interfaces*, **9**, 20833 (2017); https://doi.org/10.1021/acsami.7b04095
15. H.-C. Wu, T.-W. Wang, J.-S. Sun, Y.-H. Lee, M.-H. Shen, Z.-R. Tsai, C.-Y. Chen and H.-C. Hsu, *Materials*, **9**, 198 (2016); https://doi.org/10.3390/ma9030198
16. D.J. Buckley, M. Berger and D. Poller, *J. Polym. Sci.*, **56**, 163 (1962); https://doi.org/10.1002/pol.1962.1205616314
17. Y. Boonsongrit, H. Abe, K. Sato, M. Naito, M. Yoshimura, H. Ichikawa and Y. Fukumori, *Mater. Sci. Eng. B*, **148**, 162 (2008); https://doi.org/10.1016/j.mseb.2007.09.006
18. W. Feng, S. Feng, K. Tang, X. He, A. Jing and G. Liang, *J. Alloys Compd.*, **693**, 482 (2017); https://doi.org/10.1016/j.jallcom.2016.09.234
19. A.M. Bargan, G. Ciobanu, C. Luca, M. Diaconu and I.G. Sandu, *Mater. Plast.*, **51**, 167 (2014).
20. M. Qi, S. Qin, Y. Wang, S. Yao, L. Qi, Y. Wu, Y. Lu and F. Cui, *Crystals*, **10**, 678 (2020); https://doi.org/10.3390/cryst10080678
21. R.C. Cuozzo, S.C. Sartoretto, R.F.B. Resende, E. Mavropoulos, M.H.P. da Silva, A.T.N.N. Alves and M.D. Calasans-Maia, *J. Biomed. Mater. Res. B Appl. Biomater.*, **108**, 2610 (2020); https://doi.org/10.1002/jbm.b.34593
22. S. Devikala, D. Ajith, P. Kamaraj and M. Arthanareeswari, *Mater. Today Proc.*, **14**, 630 (2019); https://doi.org/10.1016/j.matpr.2019.04.186
23. S. Shabbir, S. Zulfiqar, M. Ishaq and M.I. Sarwar, *Colloid Polym. Sci.*, **286**, 673 (2008); https://doi.org/10.1007/s00396-007-1811-9
24. M. Krishnamoorthy, S. Hakobyan, M. Ramstedt and J.E. Gautrot, *Chem. Rev.*, **114**, 10976 (2014); https://doi.org/10.1021/cr500252u
25. K. Rajesh, V. Crasta, N.B. Rithin Kumar, G. Shetty and P.D. Rekha, *J. Polym. Res.*, **26**, 99 (2019); https://doi.org/10.1007/s10965-019-1762-0
26. J.R. Padhi, D. Nayak, A. Nanda, P.R. Rauta, S. Ashe and B. Nayak, *Carbohydr. Polym.*, **153**, 292 (2016); https://doi.org/10.1016/j.carbpol.2016.07.098
27. H. Bundela and A.K. Bajpai, *Express Polym. Lett.*, **2**, 201 (2008); https://doi.org/10.3144/expresspolymlett.2008.25
28. R. Mishra, R. Varshney, N. Das, D. Sircar and P. Roy, *Eur. Polym. J.*, **119**, 155 (2019); https://doi.org/10.1016/j.eurpolymj.2019.07.007
29. G. Yin, Z. Liu, J. Zhan, F. Ding and N. Yuan, *Chem. Eng. J.*, **87**, 181 (2002); https://doi.org/10.1016/S1385-8947(01)00248-0
30. V. Ozhukil Kollath, F. Van den Broeck, K. Fehér, J.C. Martins, J. Luyten, K. Traina, S. Mullens and R. Cloots, *Chem. Eur. J.*, **21**, 10497 (2015); https://doi.org/10.1002/chem.201500223
31. Z. He, S. Sun and C. Deng, *J. Bionics Eng.*, **17**, 345 (2020); https://doi.org/10.1007/s42235-020-0028-1
32. V.P. Padmanabhan, R. Kulandaivelu, S.N.T. Nellaiappan, S. Sagadevan, M. Lakshmipathy and M.R. Johan, *Ceram. Int.*, **46**, 2510 (2020); https://doi.org/10.1016/j.ceramint.2019.09.245
33. D.K. Pathak and P.M. Pandey, *J. Biomed. Mater. Res. B Appl. Biomater.*, **109**, 436 (2020); https://doi.org/10.1002/jbm.b.34712
34. X. Xu, N. Wang, M. Wu, J. Wang, D. Wang, Z. Chen, J. Xie, C. Ding and J. Li, *Colloids Surf. B Biointerfaces*, **194**, 111206 (2020); https://doi.org/10.1016/j.colsurfb.2020.111206
35. Y.O. Nikitina, N.V. Petrakova, A.A. Egorov, D.D. Titov, A.A. Ashmarin, S.M. Barinov and V.S. Komlev, *IOP Conf. Series Mater. Sci. Eng.*, **848**, 012061 (2020); https://doi.org/10.1088/1757-899X/848/1/012061
36. K.P. Ananth, J. Sun and J. Bai, *Int. J. Mol. Sci.*, **19**, 2340 (2018); https://doi.org/10.3390/ijms19082340